CHAPTER III

CO-OPTIMISED FRAMEWORK AND SPOT PRICING FOR COMBINED ELECTRICITY MARKET AND EMISSION MECHANISMS[1]

3.1 Chapter Overview

This chapter presents a comprehensive carbon-accounted dispatch and pricing framework that explicitly embeds short-run carbon emission costs into the electricity market-clearing process. The proposed model directly integrates environmental externalities into the objective function, enabling market prices to reflect economic and environmental costs simultaneously. The framework introduces a unified mathematical formulation applicable to single-sided and double-sided auction mechanisms, aiming to optimise power generation, minimise total system costs, and maximise social welfare while internalising carbon emission costs. The model is implemented on the IEEE 30-bus test system and solved using stochastic optimisation algorithms, PSO, BWO, GWO, and WOA.

Comparative analyses are conducted among algorithms to evaluate convergence performance, stability, and computational efficiency. Simulation results demonstrate that incorporating carbon costs within the dispatch framework leads to significant reductions in total emissions and consumer expenditures, alongside improvements in system-wide social welfare. Figure 3.1 illustrates the conceptual framework of the proposed carbon-accounted optimal power dispatch and spot pricing model, highlighting the interconnections among market participants, carbon taxation, and the optimisation process. This conceptual diagram visually summarises how the system operator incorporates carbon costs into market-clearing to derive environmentally informed spot prices.

---

[1] A portion of this chapter has been published in the *IEEE Transactions on Industry Applications (P. Muangkhiew & K. Chayakulkheeree, 2024; Muangkhiew & Chayakulkheeree, 2025).*

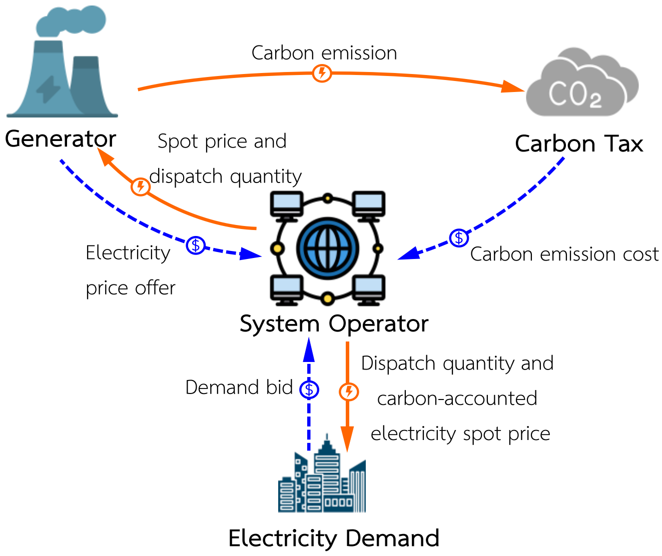

Figure 3.1 Schematic diagram of carbon-accounted optimal power dispatch and spot pricing

3.2 Mathematical Formulation

The OPF problem is a non-linear, non-convex optimisation challenge aimed at minimising specific objectives within the power system while adhering to numerous equality and inequality constraints. Mathematically, the objective function can be represented in general form as follows:

minimise $f_i(x,u)$, (3.1)

subject to $g_i(x,u)=0$, (3.2)

$h_i(x,u)\leq 0$, (3.3)

where $f_i(x,u)$ is the objective function to minimised.

In Equation (3.2), the equality constraints $g_i(x,u)$ represent the general power flow equations, which ensure the balance between power generation and demand as follows:

$$P_{G,i}-P_{L,j}-\sum_{j=1}^{NB}V_iV_j[G_{ij}\cos(\theta_i-\theta_j)+B_{ij}\sin(\theta_i-\theta_j)]=0 \quad, i=1,\ldots,NB, \tag{3.4}$$

$$Q_{G,i} - Q_{L,j} - \sum_{j=1}^{NB} V_i V_j [G_{ij} \sin(\theta_i - \theta_j) - B_{ij} \cos(\theta_i - \theta_j)] = 0 \quad , i = 1,..., NB . \tag{3.5}$$

Also, Equation (3.3) represents the inequality constraints $h_i(x,u)$ as follows:

(1) Generation constraints: Bus voltage limits $(V_{G,i})$, active power output limit $(P_{G,i})$, and reactive power output limit $(Q_{G,i})$ are restricted by their lower and upper limits as follows:

$$V_{G,i}^{\min} \le V_{G,i} \le V_{G,i}^{\max} \quad , i = 1,..., NG \ , \tag{3.6}$$

$$P_{G,i}^{\min} \le P_{G,i} \le P_{G,i}^{\max} \quad , i = 1,..., NG \ , \tag{3.7}$$

$$Q_{G,i}^{\min} \le Q_{G,i} \le Q_{G,i}^{\max} \quad , i = 1,..., NG \ . \tag{3.8}$$

(2) Transformer constraints: Transformer tap settings (T_i) are restricted by their limits as follows:

$$T_i^{\min} \le T_i \le T_i^{\max} \quad , i = 1,..., NT \ . \tag{3.9}$$

(3) Shunt reactor adjustments constraints: Shunt reactor adjustments $(Q_{C,i})$ are bouned as follows:

$$Q_{C,i}^{\min} \le Q_{C,i} \le Q_{C,i}^{\max} \quad , i = 1,..., NC . \tag{3.10}$$

(4) Security constraints: Voltages at load buses and line flow limit constraints are as follows:

$$V_{L,i}^{\min} \le V_{L,i} \le V_{L,i}^{\max} \quad , i = 1,..., NL , \tag{3.11}$$

$$S_{l,i} \le S_{l,i}^{\max} \quad , i = 1,..., nl . \tag{3.12}$$

The state variables are the dependent variables u that define the distinct state of the power system. The state variables of the OPF include the active power output of the slack bus $(P_{G,1})$, generator reactive power outputs $(Q_{G,i})$, bus voltage of load bus (V_L) , and loads of transmission line $(S_{l,i})$. The control variables or decision variables are independent variables x that can coordinate the solution of power flow equations. The control variables related to OPF are generator active power outputs $(P_{G,i})$, voltage magnitudes of generators $(V_{G,i})$, transformer tap settings (T_i), adjustment of capacitive reactance $(X_{C,i})$, and active power load $(P_{D,i})$.

3.2.1 Cost of Generation

The cost of generation (CG) can be determined as the sum of power generation in the power system using the quadratic equation. Equation (3.13) describes the generators' energy cost function regarding active power output.

$$CG(P_{G,i}) = \sum_{i=1}^{NG} (a_i P_{G,i}^2 + b_i P_{G,i} + c_i)\,, \tag{3.13}$$

where a_i, b_i and c_i are coefficients that depend on the GENCOs' willingness to sell behaviours, NG represents number of generators, $P_{G,i}$ is the active power of generators at bus i.

3.2.2 Cost of Carbon Emission

Fossil-fired generating units are significant sources of carbon emissions (CE), primarily in the form of carbon dioxide, which contributes to the accumulation of greenhouse gases and exacerbates climate change. There is a direct correlation between the power generated (in per unit MW) and the CE produced (in tons per hour, t/h) as follows:

$$CE(P_{G,i}) = \sum_{i=1}^{NG} (\alpha_i P_{G,i}^2 + \beta_i P_{G,i} + \omega_i)\,. \tag{3.14}$$

Consequently, the cost of carbon emission (CCE) for a fossil-fired generation unit can be expressed as the product of a carbon tax (C_{tax}) in dollars per ton and the total carbon emissions. This formulation reflects the actual societal cost of carbon emissions, accounting for the adverse impacts of climate change on the environment and public health. Therefore, the CCE can be mathematically represented as the product of the C_{tax} and the corresponding CE as follows:

$$CCE(P_{G,i}) = C_{tax} \times \sum_{i=1}^{NG} CE(P_{G,i}), \tag{3.15}$$

where α_i, β_i and γ_i are the coefficients of carbon emission at bus i.

3.2.3 Demand benefit

The demand benefit represents the economic value or utility that consumers derive from the consumption of electrical energy. In market models, this is often quantified by the consumers' willingness to pay. The aggregate benefit for all loads in the system can be modelled as a function of power consumption. Equation (3.16) describes the consumers' benefit function, which is commonly represented by a quadratic equation.

$$B_j(P_{D,j}) = \sum_{j=1}^{ND} (d_j P_{D,j}^2 + e_j P_{D,j} + k_j), \tag{3.16}$$

where d_j, e_j and k_j are the non-negative coefficients of the benefit function for the load at bus j, which are derived from consumer bidding behaviour. ND represents the total number of load buses, $P_{D,j}$ is the active power consumed by the load at bus j.

3.2.4 Spot Pricing of Electricity

In electricity markets, spot prices are determined using a methodology that incorporates key pricing characteristics, mainly incremental transmission losses and transmission line constraint relaxation. These factors are essential for reflecting the physical realities and limitations of the power grid and can be accurately calculated using power system sensitivity techniques (Wood & Wollenberg, 2014). Therefore, the spot price considered in this work includes the market-clearing price (MCP), marginal transmission loss, and network quality of supply, all of which can be calculated as follows (Schweppe et al., 1988):

$$\rho_i = \lambda + \eta_{L,i} + \eta_{QS,i}, \quad i = 1,...,NB, \tag{3.17}$$

$$\eta_{L,i} = \lambda \times (-ITL_i), \quad i = 1,...,NB, \tag{3.18}$$

$$\eta_{QS,i} = -\sum_{l=1}^{NB} \mu_l (a_{li}), \quad i = 1,...,NB, \tag{3.19}$$

where ρ_i is the spot price at bus i (\$/MWh); λ is the system marginal price (\$/MWh); $\eta_{L,i}$ is marginal transmission loss at bus i (\$/MWh); $\eta_{QS,i}$ is network quality of supply at bus i (\$/MWh); ITL_i is the incremental transmission loss; μ_l is the reduction in supply cost that results from an incremental relaxation of constraint l (\$/MWh); a_{li} is the line l sensitivity factor to the active injection power at bus i, NB is the total number of buses.

The marginal loss component is calculated using the Jacobian matrix from the Newton-Raphson power flow (NRPF) method. In this method, the changes in active and reactive power injections are determined by analysing the power flow equations as follows:

$$\begin{bmatrix} dP \\ dQ \end{bmatrix} = \begin{bmatrix} \frac{\partial P}{\partial \delta} & \frac{\partial P}{\partial v} \\ \frac{\partial Q}{\partial \delta} & \frac{\partial Q}{\partial v} \end{bmatrix} \begin{bmatrix} d\delta \\ dv \end{bmatrix}. \tag{3.20}$$

Specifically, the change in injection power at the S-th slack bus as follows:

$$dP_S = \left[\frac{\partial P_S}{\partial \delta} \right] [d\delta], \tag{3.21}$$

since $\frac{\partial P}{\partial v} \approx 0$ and $\frac{\partial Q}{\partial \delta} \approx 0$, so

$$dP_S = \left[\frac{\partial P_S}{\partial \delta} \right] \left[\frac{\partial P}{\partial \delta} \right]^{-1} [dP] = [\gamma_1, \gamma_2, ..., \gamma_{S-1}, \gamma_{S+1}, ..., \gamma_{NB}][dP]. \tag{3.22}$$

The change in total active power loss can be derived from these calculations as follows:

$$dP_{loss} = dP_S + \sum_{\substack{i=1 \\ i \neq S}}^{NB} dP_i \ = \sum_{\substack{i=1 \\ i \neq S}}^{NB} (1-\gamma_i) dP_i \ . \tag{3.23}$$

The incremental transmission loss (ITL_i) is a sensitivity factor that quantifies the impact of incremental changes in active power injection at bus i on the total system losses. Mathematically, ITL_i is defined as the partial derivative of the total system losses for the active power injection at bus i. This relationship is expressed in the following equation.

$$ITL_i = \frac{dP_{loss}}{dP_i} = 1 + \gamma, \quad i = 1,\ldots, S-1, S+1,\ldots, NB \tag{3.24}$$

and $ITL_S = 0$.

Consequently, the change in system losses due to a variation in active power load $(P_{D,i})$ at bus i can be formulated as follows:

$$\frac{dP_{loss}}{dP_{D,i}} = -ITL_i \ , \tag{3.25}$$

where P_{loss} represents the total system active power loss.

3.2.5 Social Welfare Formulation

Social welfare (SW) within electricity markets encapsulates the holistic societal advantage of energy production and consumption. It is represented as the disparity between the value of energy to society, gauged by society's willingness to pay for its demand, and the expenses incurred in energy production and distribution. SW is a composite of generation costs and consumer benefits. Maximising SW necessitates optimising consumer benefits while concurrently minimising power generation costs. So, the general form of SW is formulated as:

$$SW = \sum_{j=1}^{ND} B_j(P_{D,j}) - \sum_{i=1}^{NG} C_i(P_{G,i}) \,, \tag{3.26}$$

where $B_j(P_{D,j})$ denotes the consumers willing to buy at the price at load bus j, ND represents the total number of loads.

3.3 Objective Function and Study Cases

The study investigates two different auction schemes: single-sided auction (SSA) and double-sided auction (DSA). The SSA scheme investigates the impact of integrating carbon emission costs into the spot pricing of electricity. On the other hand, the DSA scheme evaluates the effects of carbon emission costs on the welfare of society. This study aims to provide a comprehensive analysis of the impact of carbon emission costs on the electricity market, considering supply-side and demand-side behaviour by implementing these two auction mechanisms. The summary of case studies in this chapter is shown in Table 3.1.

Table 3.1 The summary of case studies in Chapter 3

Cases	**Spot pricing**		**Demand-side bidding**	**Social welfare**
	Electricity	*Carbon emission*		
Case 3.1a	✓			
Case 3.1b	✓	✓		
Case 3.2a	✓		✓	✓
Case 3.2b	✓	✓	✓	✓

3.3.1 Scheme 1: Single-Side Auction Scheme

Case 3.1a: Conventional Single-Side Auction Scheme

This case study involves the conventional electricity spot market, which determines electricity pricing without accounting for carbon emissions pricing mechanisms. Consequently, the objective function to be minimised is formulated as follows:

minimise $$f_{3.1\text{a}}(x,u)=\sum_{i=1}^{NG}CG(P_{G,i})+\mu\cdot\left[g(x,u)\right]^2, \tag{3.27}$$

subject to equality and inequality constraints as in Equations (3.4)-(3.12), where $CG(P_{G,i})$ is formulated as shown in Equation (3.13), μ denotes the penalty factor, and $\left[g(x,u)\right]^2$ represents the quadratic penalty term.

Case 3.1b: Carbon-accounted Single-Side Auction Scheme

In this case, the pricing mechanism for electricity incorporates a cost component that accounts for the carbon emissions associated with power generation. Thus, the objective function for this case can be formulated as follows:

minimise $$f_{3.1\text{b}}(x,u)=\left[\sum_{i=1}^{NG}CG(P_{G,i})+\sum_{i=1}^{NG}CCE(P_{G,i})\right]+\mu\cdot\left[g(x,u)\right]^2, \tag{3.28}$$

subject to equality and inequality constraints as in Equations (3.4)-(3.12), where $CCE(P_{G,i})$ is formulated as shown in Equation (3.15).

3.3.2 Scheme 2: Double-Side Auction Scheme

Case 3.2a: Conventional Double-Side Auction Scheme

This case aims to maximise the overall social welfare, disregarding the CCE associated with power generation. The formulation incorporates the electricity offer prices submitted by GENCOs and the demand-side bidding (DSB) mechanism facilitated by DISCOs. Hence, the objective function can be expressed as follows:

maximise $$f_{3.2\text{a}}=\left[\sum_{j=1}^{ND}B_j(P_{D,j})-\sum_{i=1}^{NG}CG(P_{G,i})\right]+\mu\cdot[g(x,u)]^2, \tag{3.29}$$

subject to equality and inequality constraints as in Equations (3.4)-(3.12).

Case 3.2b: Carbon-accounted Double-Side Auction Scheme

This case aims to maximise the overall social welfare for electricity offer prices, accounting for CCE and the demand-side bidding mechanism. Hence, the objective function can be formulated as follows:

maximise $$f_{3.2\mathrm{b}} = \left[\sum_{j=1}^{ND} B_j(P_{D,j}) - \sum_{i=1}^{NG} CG(P_{G,i}) - \sum_{i=1}^{NG} CCE(P_{G,i}) \right] + \mu \cdot \left[g(x,u) \right]^2, \quad (3.30)$$

subject to equality and inequality constraints as in Equations (3.4)-(3.12).

For Cases 3.1a and 3.2a, the spot prices are determined based on electricity generation costs, excluding costs associated with carbon emissions, which can be calculated as Equation (3.31). Additionally, the CCE calculated using Equation (3.15) is combined with the products of electricity consumption and spot prices, which can be formulated as Equation (3.32).

$$\rho_i^{wo} = \lambda_{CG} + \eta_{L,i} + \eta_{QS,i} \quad , i = 1,\ldots,NB, \quad (3.31)$$

$$EC_i^{wo} = (\rho_i^{wo} \times P_{D,i}) + CCE(P_{G,i}) \quad , i = 1,\ldots,NB. \quad (3.32)$$

Conversely, in Cases 3.1b and 3.2b, the carbon emissions cost was incorporated into the spot pricing mechanism, which can be calculated as Equation (3.33). Under carbon-accounted spot pricing, the electricity cost (EC) is the power product and the corresponding carbon-accounted spot price. Mathematically, it can be expressed in Equation (3.34).

$$\rho_i^{w} = (\lambda_{CG} + \lambda_{CCE}) + \eta_{L,i} + \eta_{QS,i} \quad , i = 1,\ldots,NB, \quad (3.33)$$

$$EC_i^{w} = \rho_i^{w} \times P_{D,i} \quad , i = 1,\ldots,NB. \quad (3.34)$$

Therefore, the total cost to consumers (TCC) can be formulated in general terms as follows:

$$TCC = \sum_{i=1}^{NB} EC_i^{wo} \text{ or } \sum_{i=1}^{NB} EC_i^{w}. \quad (3.35)$$

3.4 Methodology

The proposed optimisation algorithm incorporates carbon emission prices into the OPF framework. The primary goal is to maximise electricity generation, reduce environmental costs, and maximise social welfare while assessing the effectiveness of various auction schemes and optimisation approaches. The PSO (Kennedy & Eberhart, 1995) results are compared with those from BWO (Hayyolalam & Pourhaji Kazem, 2020), GWO (Mirjalili et al., 2014), and WOA (Mirjalili & Lewis, 2016). The proposed approach's conceptual flowchart, illustrated in Figure 3.2, is based on carbon-accounted optimal power dispatch and spot pricing approach.

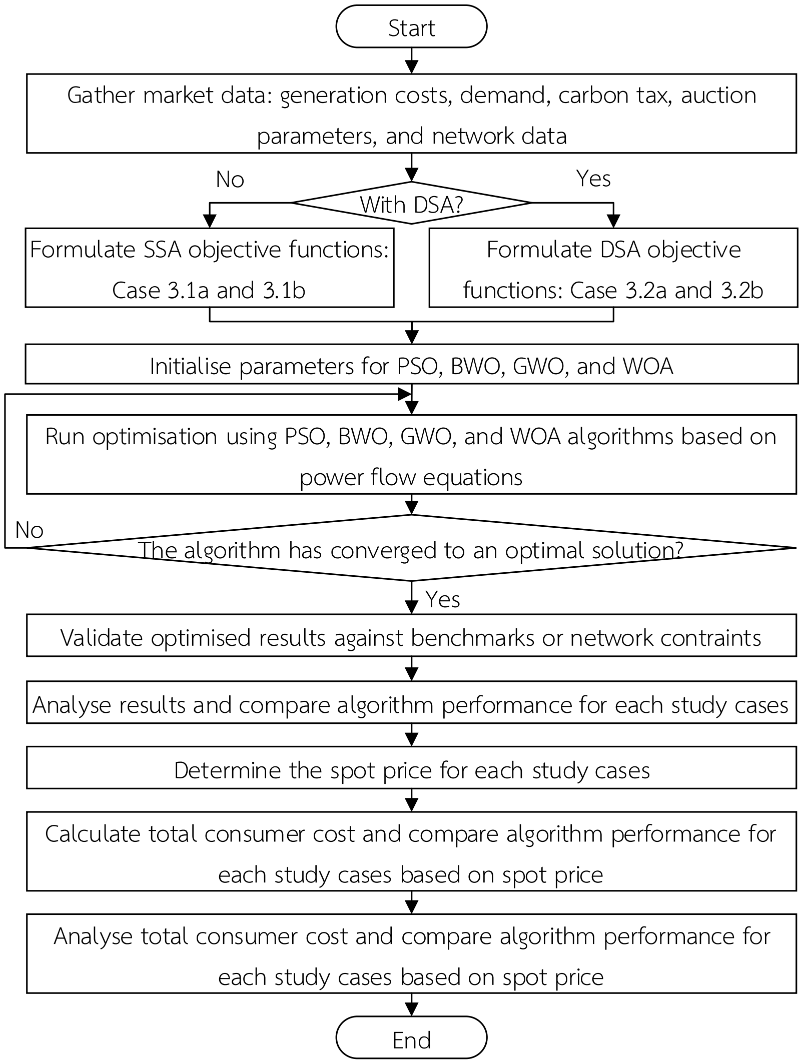

Figure 3.2 The proposed carbon-accounted optimal power dispatch and spot pricing flowchart

The vector population, representing the control variables x, for the single-side auction and double-side auction schemes, are defined to enhance the search for the best value as:

$$\mathbf{x} = [x_1,\ x_2,\ \dots,\ x_{NP}]\ ,\ i = 1,\dots,NP\ , \tag{3.36}$$

where NP is the number of particles in the population.

The Variable search boundaries include generation limits, voltage constraints, transformer tap settings, and reactive power compensation ranges, all defined based on IEEE standard test systems.

From the formulation,

(1) Single-Side Auction Scheme

$$\mathbf{x} = [P_{G,2} \dots P_{G,NG},\ V_{G,1} \dots V_{G,NG},\ T_1 \dots T_{NT},\ X_{C,1} \dots X_{C,NC}], \tag{3.37}$$

(2) Double-Side Auction Scheme

$$\mathbf{x} = [P_{G,2} \dots P_{G,NG}, V_{G,1} \dots V_{G,NG}, T_1 \dots T_{NT}, X_{C,1} \dots X_{C,NC}, P_{D,j} \dots P_{D,ND}], \tag{3.38}$$

where $P_{G,i}$ denotes active power output of the generator at bus i, $V_{G,i}$ is voltage magnitude for the generator bus i, T_i is tap setting limits for the transformer i, $X_{C,i}$ is reactance control setting of the shunt reactor i, and $P_{D,j}$ is active power demand at bus j.

The boundaries of the Variables are the power generation limit, voltage limit, transformer tap settings, and reactive power compensation ranges. For the IEEE 30-bus test system, the power generation limits are provided in Table A.1, while the transformer tap settings and voltage levels are constrained within the range of [0.90 1.10]. This chapter compares PSO proposed method to BWO, GWO, and WOA, so the computation algorithms are as follows:

Step computation of PSO

Step 1: Initialise a swarm of particles with random positions and velocities according to Equation (3.36). Each particle represents a candidate solution within the search space.

Step 2: Evaluate the fitness value of each particle using the objective function.

Step 3: Assign each particle's current position as its personal best ($pbest$), and determine the global best position ($gbest$) among all particles.

Step 4: Update the velocity of each particle based on the cognitive and social components that depend on $pbest$ and $gbest$.

Step 5: Update each particle's position using the newly computed velocity.

Step 6: Recalculate the fitness value of each particle and update both $pbest$ and $gbest$ better solutions are found.

Step 7: Repeat Steps 4-6 until the predefined stopping criterion, such as the maximum number of iterations, is satisfied.

Step 8: Return the final $gbest$ as the optimal solution.

Step computation of BWO

Step 1: Initialise the population of search agents randomly using Equation (3.36).

Step 2: Set the maximum number of iterations and initialise pheromone values for all agents.

Step 3: Randomly generate two control Variables: $m \in [0.4, 0.9]$ and $\beta \in [-1.0, 1.0]$

Step 4: For each search agent, update its position based on a random probability threshold (0.3).

- If $rand < 0.3$, update position using the first update rule.
- Otherwise, update position using the second update rule.

Step 5: Compute the pheromone value for each agent based on its fitness.

Step 6: Identify and update agents with $pheromone \leq 0.3$ to enhance exploration.

Step 7: Evaluate the fitness of all agents after position updates.

Step 8: Apply the survival (σ) procedure:

- If $rand \leq 0.5$, discard the agent; otherwise, retain it.

Step 9: Update the best agent if a better fitness value is obtained.

Step 10: Repeat Steps 3-9 until the maximum iteration limit is reached.

Step 11: Return the best agent as the final optimal solution.

where m is a mating ratio, a randomly chosen value between 0.4 and 0.9 that determines the offspring creation; $pheromone_i$ is a fitness indicator used to evaluate the quality of a solution. β is a random number in the range [-1, 1] used for updating the positions in oscillation-based movements. σ is the survival probability, deciding whether offspring survive or are eliminated.

Step computation of GWO

Step 1: Initialise a population of wolves with random positions using Equation (3.36).

Step 2: Evaluate the fitness of all wolves and identify the three best individuals, denoted as x_α (best), x_β (second best), and x_γ (third best).

Step 3: For each iteration, update the coefficient vectors and compute the distance of each wolf relative to x_α, x_β, and x_γ using the GWO position update equations.

Step 4: Update each wolf's position based on the encircling and hunting behaviour determined by x_α, x_β, and x_γ.

Step 5: Evaluate the updated fitness values of all wolves and adjust x_α, x_β, and x_γ according to the new rankings.

Step 6: Repeat Steps 3-5 until the termination criterion, such as the maximum iteration limit, is satisfied.

Step 7: Return the position of x_α as the final optimal solution.

where x_α is the position of the alpha wolf, representing the best solution. x_β is the position of the beta wolf, representing the second-best solution. x_δ is the position of the delta wolf, representing the third-best solution. A is a coefficient vector that decreases linearly from 2 to 0, balancing exploration and exploitation. C is a coefficient vector with random values in the range [0, 2], controlling the influence of leader wolves on the rest.

Step computation of WOA

Step 1: Initialise the whale population randomly using Equation (3.36).

Step 2: Evaluate the fitness of each whale and identify the best whale as the leader.

Step 3: For each iteration, update the control Variables a, A, C, l and p.

Step 4: If $p < 0.5$:

- If $|A| < 1$, update each whale's position toward the best solution (exploitation phase).
- If $|A| \geq 1$, select a random whale and update the position to explore new regions (exploration phase).

Step 5: If $p \geq 0.5$, update the whale's position using a spiral motion toward the best solution, mimicking bubble-net hunting behaviour.

Step 6: Evaluate the fitness of all whales and update the best whale if a superior solution is found.

Step 7: Repeat Steps 3-6 until the maximum iteration criterion is satisfied.

Step 8: Return the final leader whale's position as the optimal solution.

where A is a coefficient vector updated at each iteration, controlling the encircling mechanism. C is a coefficient vector that determines the weight of the leader's position in updating other whales. b is spiral shape constant, used to model the spiral position update. l is a random number in [-1, 1], defining the logarithmic spiral's randomness. p is a probability value in [0, 1], controlling the balance between encircling prey and the spiral movement.

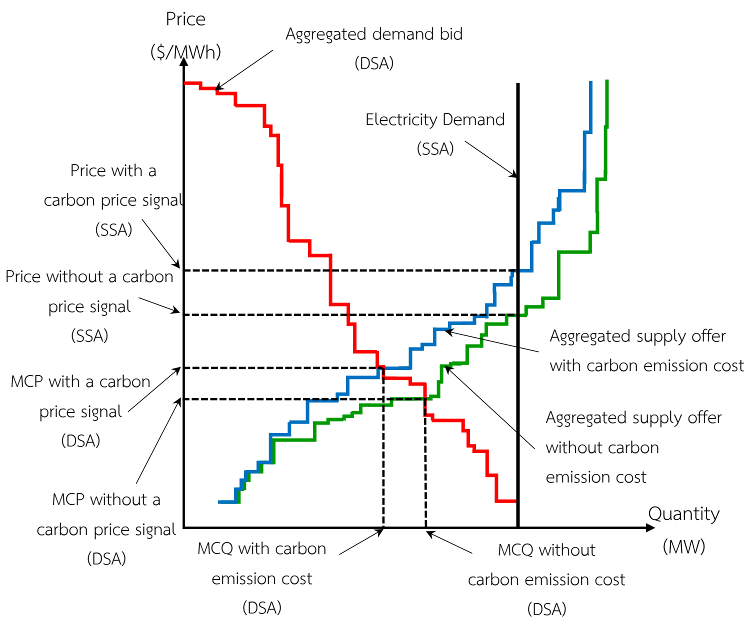

Figure 3.3 Aggregated bid curve and electricity demand

The relation between the supply and demand curves for each scheme in SSA and DSA is shown in Figure 3.3. The increased marginal costs of power generation, considering carbon emissions, are shown in the aggregated carbon-accounted supply curve. The possible differences in market-clearing prices and quantities when carbon emission costs are internalised within the electricity market are highlighted explicitly by the divergence between the demand curve's intersections and the two supply curves.

3.5 Simulation Results and Discussions

The chapter model has been tested on the IEEE 30-bus system, which includes seventeen control variables: four transformer tap settings, two shunt VAR compensators, five active power outputs of generators, and six voltage magnitudes of generators. The generation cost and carbon emission coefficients are detailed in Table A.1. In this chapter, the economic impact of greenhouse gas emissions is assessed by assuming a carbon tax (C_{tax}) of \$31 per metric ton. This subsection presents a comparative analysis of results obtained through four optimisation algorithms: PSO, BWO, GWO, and WOA, focusing on both SSA and DSA schemes.

This chapter analyses the four algorithms by comparing SSA and DSA results, followed by a statistical evaluation and case-specific analyses. The detailed parameter adjustments for each algorithm are presented in Table 3.2. Specifically, for PSO, the inertia weight (w) varied from 0.1 to 1.1, and the swarm size was set to 500. All four stochastic algorithms employed the same maximum iteration number of 1500 to ensure fair comparisons. After these analyses, optimal hyperparameters that provided the best balance of accuracy, convergence speed, and robustness were selected. Each algorithm was then executed 30 times using these optimal hyperparameters to validate the consistency and stability of the obtained solutions. The detailed parameter adjustments for each algorithm are shown in Figure B.1.

Table 3.3 presents the results of four optimisation algorithms, including PSO, BWO, GWO, and WOA, applied to the SSA scheme. The comparison shows that PSO performs most efficiently across objective functions, achieving the lowest generation cost of 799.31549 \$/h in Case 3.1a, which does not account for carbon emissions. As a result, the TCC is \$ 1,140.1179 /h. While carbon emission costs are incorporated in

Case 3.1b, PSO maintains its lead with an objective value of \$809.40759/h, reducing TCC by \$1,135.6748/h and simultaneously lowering carbon emissions compared to Case 3.1a.

Table 3.2 The best optimal hyperparameters

Algorithm	The Best Optimal Hyperparameters			
	Case 3.1a	Case 3.1b	Case 3.2a	Case 3.2b
PSO	c_1=2, c_2=1.49	c_1=1.49, c_2=1	c_1=1.49, c_2=1.49	c_1=1.49, c_2=1.49
BWO	Population size=100	Population size=80	Population size=80	Population size=80
GWO	Population size=40	Population size=40	Population size=50	Population size=40
WOA	Population size=50	Population size=60	Population size=40	Population size=60

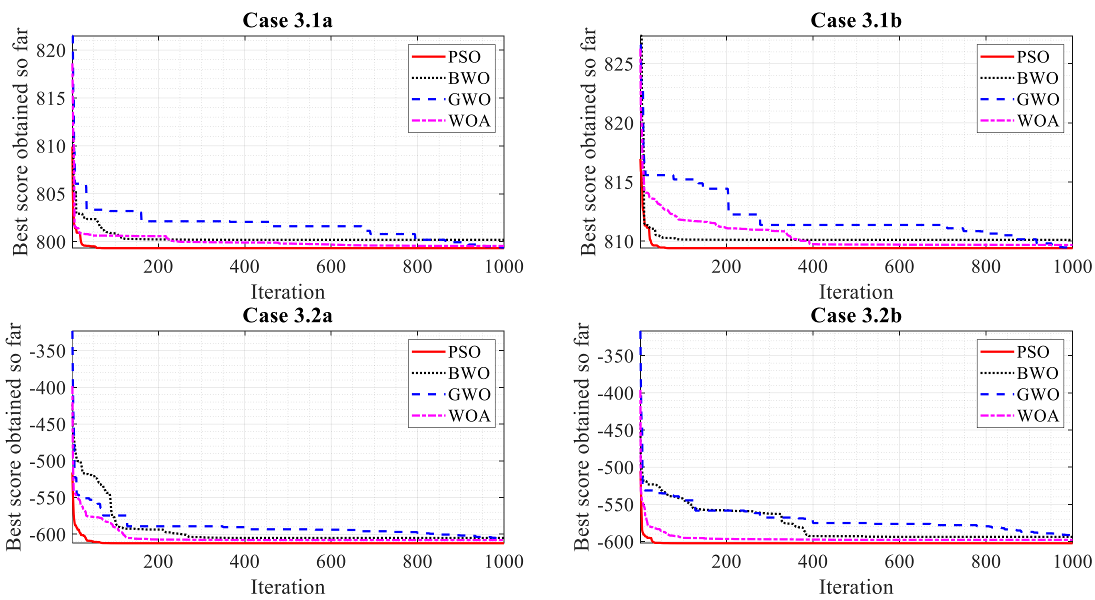

Figure 3.4 The convergence plot of the proposed method across different case studies

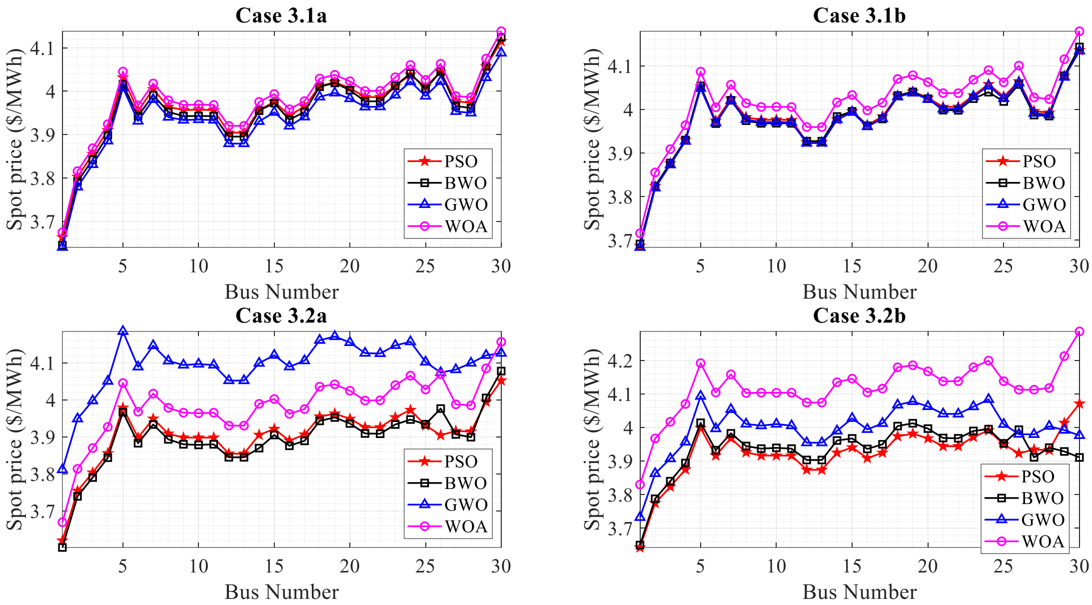

Figure 3.5 Comparison of spot prices across different case studies

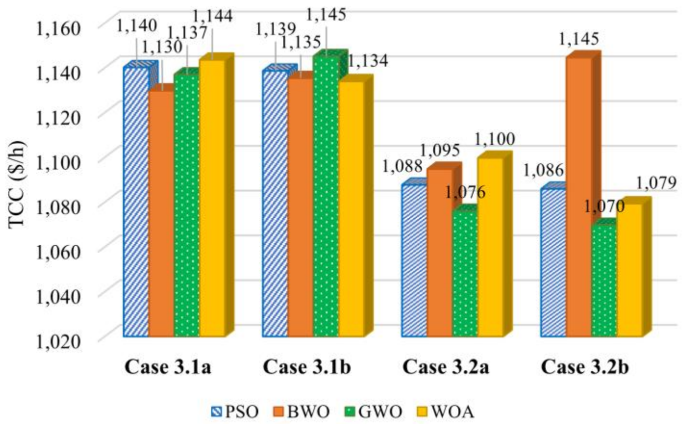

Figure 3.6 Electricity prices in different market mechanisms

Table 3.4 compares the DSA schemes of four optimisers. In this scheme, demand and supply bids are considered, and carbon costs are integrated. In Case 3.2a, which does not include carbon cost, PSO achieves the highest SW of 612.25805. Case 3.2b, accounting for carbon emissions, demonstrates significant emission reductions, with PSO registering 0.31577 tons/h of CE. This results in a TCC of 1,083.0282 $/h, lower than that of Case 3.2a. While PSO again emerges as the best-performing algorithm in the objective function of cost, emissions, and social welfare, BWO and GWO show more competitive results in terms of TCC, which indicates that these algorithms may offer slight advantages in different market conditions.

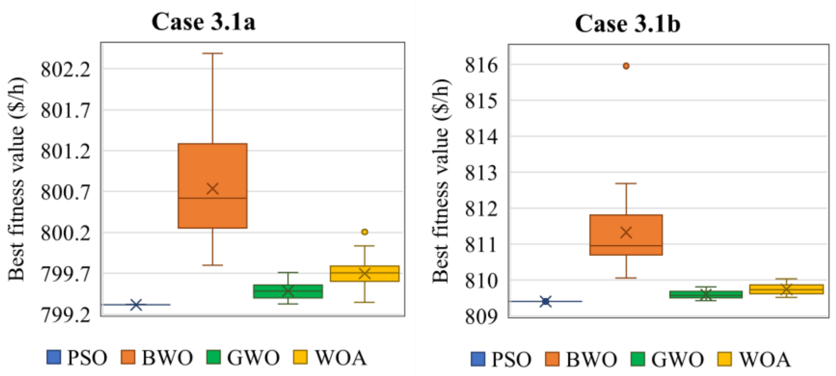

(a) Box plots for different optimisation algorithms of SSA

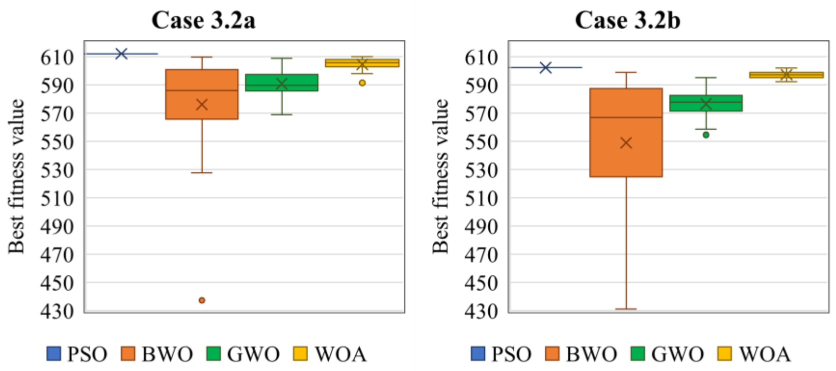

(b) Box plots for different optimisation algorithms of DSA

Figure 3.7 Statistical comparison of case studies in different optimisation algorithms

Table 3.5 summarises the best, worst, average, median, and standard deviation results for each algorithm under the SSA and DSA schemes. PSO consistently yields the best results across both auction types, particularly in minimising costs and maximising social welfare. The standard deviations of the results for PSO are the lowest, and it significantly outperforms other algorithms, further highlighting its reliability. In contrast, BWO and WOA exhibit higher variability, especially in Case 3.2b, where the worst outcomes notably impact TCC and CE. The results underline PSO’s robustness for optimising power dispatch when considering carbon emissions and spot pricing.

Figure 3.4 illustrates the convergence plots of the proposed method across different case studies. PSO demonstrates rapid convergence in all cases, comparing BWO, GWO, and WOA, typically reaching near-optimal solutions within the first 50-100 iterations. This fast convergence is particularly evident in the SSA cases (3.1a and 3.1b).

The DSA cases (3.2a and 3.2b) show slightly slower convergence, which can be attributed to the increased complexity of the problem due to the inclusion of DSB. Figure 3.5 compares spot prices across different case studies and shows the impact of carbon accounting on electricity pricing. The carbon-accounted cases (3.1b and 3.2b) generally show higher spot prices compared to their non-carbon-accounted counterparts (3.1a and 3.2a). This increase reflects the internalisation of environmental costs into the electricity market. The DSA scheme (Cases 3.2a and 3.2b) tends to result in lower and more stable spot prices compared to the SSA, likely due to the increased competition and flexibility introduced by DSB. Figure 3.6 demonstrates the effects of carbon pricing and different market mechanisms on electricity prices.

The main driver of cost optimisation in this chapter framework is the electricity price, which is influenced by various market factors, including generation costs, carbon pricing, and supply-demand dynamics. To illustrate this, a figure is provided that shows electricity price variations across different scenarios, highlighting the impact of carbon accounting and optimisation strategies on market-clearing prices. The effects of carbon pricing and other market mechanisms on electricity prices are demonstrated in Figure 3.7.

The interplay between optimisation algorithms, auction mechanisms, and carbon accounting, as revealed in these results, underscores the complex dynamics in modern electricity markets. The superior performance of PSO in terms of convergence speed suggests its potential as an efficient tool for market clearing in real-time operations. Meanwhile, the observed price differentials between carbon-accounted and non-carbon-accounted scenarios emphasise the significant role of environmental policy in shaping market outcomes. The stabilising effect of DSA on spot prices further underscores the potential benefits of increased demand-side participation in electricity markets, indicating a more balanced and efficient market design. Figure 3.8 shows the average computation times across 30 trials for each algorithm in all four scenarios. PSO required the quickest calculation time while maintaining an excellent solution quality, exceeding BWO, GWO, and WOA.

The interplay between optimisation algorithms, auction procedures, and carbon accounting, as demonstrated by these findings, highlights the complex dynamics of modern power markets. PSO's superior convergence speed shows that it could be an effective instrument for market clearing in real-time operations. Meanwhile, the observed price differences between carbon-accounted and non-carbon-accounted scenarios highlight the importance of environmental policy in determining market results. DSA's stabilising effect on spot prices emphasises the potential benefits of expanded demand-side participation in electricity markets, implying a more balanced and efficient market design.

The detailed comparison analysis confirms this, demonstrating that the suggested technique consistently produces high-quality solutions with competitive performance across various case studies. Furthermore, the consistency of the results was checked across numerous runs to reduce the impact of random fluctuation. While exact global optimality is not guaranteed due to the nature of heuristic approaches, the close performance of this solution to the theoretical optimal and its stability across trials strongly suggest that the method achieves near-global optimal solutions.

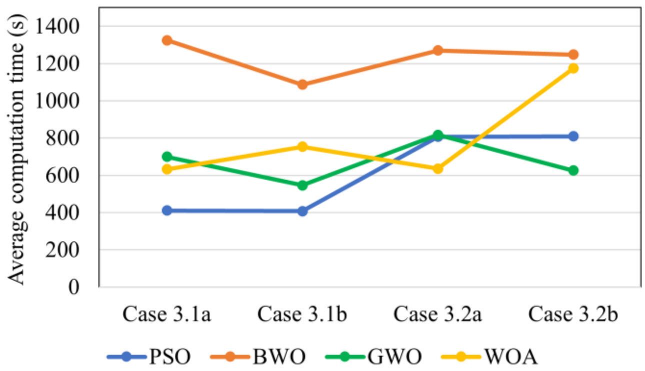

Figure 3.8 The average computation times of case studies with different optimisation algorithms

Table 3.3 Comparing the best results in different optimisation algorithms of SSA scheme

Single-Side Auction Scheme									
Variable	***Case 3.1a***				*Variable*	***Case 3.1b***			
	PSO	*BWO*	*GWO*	*WOA*		*PSO*	*BWO*	*GWO*	*WOA*
$P_{G,1}$ (MW)	177.07365	179.59219	177.96393	177.75830	$P_{G,1}$ (MW)	173.49890	169.24676	173.06652	174.13876
$P_{G,2}$ (MW)	48.70373	48.87309	48.51264	48.84775	$P_{G,2}$ (MW)	49.42987	48.99243	49.43309	49.48108
$P_{G,5}$ (MW)	21.30557	21.15851	21.12053	21.39806	$P_{G,5}$ (MW)	21.57253	21.06155	21.54725	21.80406
$P_{G,8}$ (MW)	21.10103	18.66231	20.77375	21.13008	$P_{G,8}$ (MW)	22.75124	26.78892	23.08085	21.73904
$P_{G,11}$ (MW)	11.91005	11.66530	11.76984	11.03133	$P_{G,11}$ (MW)	12.59854	12.88982	12.66577	12.54806
$P_{G,13}$ (MW)	12.00000	12.56332	12.03073	12.04303	$P_{G,13}$ (MW)	12.00001	12.68169	12.03379	12.25912
$V_{G,1}$ (p.u.)	1.10000	1.10000	1.10000	1.10000	$V_{G,1}$ (p.u.)	1.10000	1.10000	1.10000	1.10000
$V_{G,2}$ (p.u.)	1.08781	1.09872	1.08760	1.08919	$V_{G,2}$ (p.u.)	1.08802	1.08687	1.08799	1.08957
$V_{G,5}$ (p.u.)	1.06176	1.07048	1.06121	1.06191	$V_{G,5}$ (p.u.)	1.06210	1.06498	1.06218	1.06558
$V_{G,8}$ (p.u.)	1.06920	1.07725	1.06814	1.07215	$V_{G,8}$ (p.u.)	1.06984	1.07157	1.07000	1.06866
$V_{G,11}$ (p.u.)	1.10000	1.10000	1.06330	1.08498	$V_{G,11}$ (p.u.)	1.10000	1.09999	1.10000	1.08957
$V_{G,13}$ (p.u.)	1.10000	1.05514	1.10000	1.09036	$V_{G,13}$ (p.u.)	1.10000	1.10000	1.09978	1.08957
T_1 (p.u.)	1.08107	1.10000	1.09555	0.99843	T_1 (p.u.)	1.08333	0.98480	1.02594	0.98422
T_2 (p.u.)	0.91209	1.07594	0.92279	0.99790	T_2 (p.u.)	0.90944	1.02770	0.99774	1.05383
T_3 (p.u.)	0.96816	1.05666	0.94297	0.99613	T_3 (p.u.)	0.96747	1.05219	0.98649	1.05332
T_4 (p.u.)	0.95808	1.02773	0.95060	0.99844	T_4 (p.u.)	0.95801	1.01302	0.97227	0.98983

Table 3.3 Comparing the best results in different optimisation algorithms of SSA scheme (Continued)

Single-Side Auction Scheme									
Variable	***Case 3.1a***				*Variable*	***Case 3.1b***			
	PSO	*BWO*	*GWO*	*WOA*		*PSO*	*BWO*	*GWO*	*WOA*
$X_{C,1}$ (p.u.)	-3.71260	-11.33756	-2.28701	-7.75570	$X_{C,1}$ (p.u.)	-3.71014	-22.04395	-4.24223	-8.75058
$X_{C,2}$ (p.u.)	-9.88323	-8.19291	-7.78196	-8.25301	$X_{C,2}$ (p.u.)	-9.90088	-20.33743	-10.09805	-11.32186
$\boldsymbol{f_{3.1a}}$ (\$/h)	**799.31549**	800.19211	799.37519	799.55243	$\boldsymbol{f_{3.1b}}$ (\$/h)	**809.40759**	810.11192	809.43595	809.68000
CE (t/h)	0.32904	0.33390	0.33078	0.33053	*CE (t/h)*	0.32216	0.31408	0.32133	0.32329
CCE (\$/h)	10.20031	10.35105	10.25421	10.24650	*CCE (\$/h)*	9.98693	9.73650	9.96115	10.02194
TCC (\$/h)	1,140.1178	1,137.3258	1,133.4391	1,144.3921	*TCC (\$/h)*	1,135.6747	1,135.1834	1,134.5692	1,145.2994

Table 3.4 Comparing the best results in different optimisation algorithms of DSA scheme

Double-Side Auction Scheme									
Variable	*Case 3.2a*				*Variable*	*Case 3.2b*			
	PSO	*BWO*	*GWO*	*WOA*		*PSO*	*BWO*	*GWO*	*WOA*
$P_{G,1}$ (MW)	172.47011	170.24654	166.50682	175.33804	$P_{G,1}$ (MW)	168.98342	168.31714	162.57575	159.17631
$P_{G,2}$ (MW)	47.59365	48.32202	45.90390	48.68086	$P_{G,2}$ (MW)	48.29905	47.94210	45.42560	45.71099
$P_{G,5}$ (MW)	20.96051	20.42179	19.41160	21.35615	$P_{G,5}$ (MW)	21.21893	21.27578	19.09130	20.51258
$P_{G,8}$ (MW)	18.38719	19.70981	12.99476	17.86595	$P_{G,8}$ (MW)	20.00595	12.18542	12.24699	35.00000
$P_{G,11}$ (MW)	10.94443	10.54262	11.25003	11.59527	$P_{G,11}$ (MW)	11.61811	12.59673	10.43534	10.00000
$P_{G,13}$ (MW)	12.00000	12.02866	16.23014	12.00000	$P_{G,13}$ (MW)	12.00000	13.14655	14.89551	12.00000
$V_{G,1}$ (p.u.)	1.10000	1.10000	1.09964	1.10000	$V_{G,1}$ (p.u.)	1.10000	1.10000	1.10000	1.10000
$V_{G,2}$ (p.u.)	1.08793	1.10000	1.08818	1.10000	$V_{G,2}$ (p.u.)	1.08814	1.10000	1.08708	1.10000
$V_{G,5}$ (p.u.)	1.06202	1.10000	1.06263	1.10000	$V_{G,5}$ (p.u.)	1.06235	1.10000	1.06228	1.08132
$V_{G,8}$ (p.u.)	1.06985	1.10000	1.07274	1.10000	$V_{G,8}$ (p.u.)	1.07048	1.10000	1.06995	1.10000
$V_{G,11}$ (p.u.)	1.09995	1.10000	1.00070	1.10000	$V_{G,11}$ (p.u.)	1.09125	1.10000	1.07253	1.10000
$V_{G,13}$ (p.u.)	1.10000	1.10000	1.09543	1.10000	$V_{G,13}$ (p.u.)	1.10000	1.10000	1.06448	1.10000
T_1 (p.u.)	1.05675	1.10000	1.07627	1.10000	T_1 (p.u.)	1.05505	1.10000	1.03733	1.10000
T_2 (p.u.)	0.93730	1.10000	0.92813	1.10000	T_2 (p.u.)	0.94329	1.10000	0.97980	1.10000
T_3 (p.u.)	0.96778	1.10000	1.09474	1.10000	T_3 (p.u.)	0.96721	1.10000	1.05536	1.10000
T_4 (p.u.)	0.95984	1.10000	1.02986	1.10000	T_4 (p.u.)	0.95982	1.10000	1.02457	1.10000

Table 3.4 Comparing the best results in different optimisation algorithms of DSA scheme (Continued)

Double-Side Auction Scheme									
Variable	*Case 3.2a*				*Variable*	*Case 3.2b*			
	PSO	*BWO*	*GWO*	*WOA*		*PSO*	*BWO*	*GWO*	*WOA*
$X_{C,1}$ (p.u.)	-3.72698	-45.00000	-6.14379	-5.77242	$X_{C,1}$ (p.u.)	-3.37395	-4.09873	-6.74545	-6.50684
$X_{C,2}$ (p.u.)	-10.02087	-45.00000	-18.26346	-8.00074	$X_{C,2}$ (p.u.)	-10.02062	-33.86133	-7.93134	-7.96603
$P_{D,2}$ (MW)	21.70000	21.70000	21.69906	21.70000	$P_{D,2}$ (MW)	21.70000	21.70000	21.70000	21.70000
$P_{D,3}$ (MW)	2.40000	2.39999	2.35116	2.40000	$P_{D,3}$ (MW)	2.40000	2.40000	2.26811	2.40000
$P_{D,4}$ (MW)	7.60000	7.59686	7.59693	7.60000	$P_{D,4}$ (MW)	7.60000	7.60000	7.59965	7.60000
$P_{D,5}$ (MW)	94.20000	94.20000	94.20000	94.20000	$P_{D,5}$ (MW)	94.20000	94.20000	94.20000	94.20000
$P_{D,7}$ (MW)	22.80000	22.80000	22.80000	22.80000	$P_{D,7}$ (MW)	22.80000	22.80000	22.79939	22.80000
$P_{D,8}$ (MW)	30.00000	30.00000	29.98738	30.00000	$P_{D,8}$ (MW)	30.00000	30.00000	30.00000	30.00000
$P_{D,10}$ (MW)	0.00000	0.13230	0.69572	0.10162	$P_{D,10}$ (MW)	0.00000	0.00000	0.95975	0.25024
$P_{D,12}$ (MW)	11.20000	11.20000	11.20000	11.20000	$P_{D,12}$ (MW)	11.20000	11.20000	11.20000	11.20000
$P_{D,14}$ (MW)	6.20000	0.83952	4.34958	6.20000	$P_{D,14}$ (MW)	6.20000	6.20000	3.01190	6.20000
$P_{D,15}$ (MW)	8.20000	8.19998	8.19873	8.20000	$P_{D,15}$ (MW)	8.20000	8.20000	8.19035	8.20000
$P_{D,16}$(MW)	3.50000	3.50000	3.49289	3.50000	$P_{D,16}$(MW)	3.50000	3.50000	3.49857	3.50000
$P_{D,17}$ (MW)	9.00000	9.00000	8.50449	9.00000	$P_{D,17}$ (MW)	9.00000	9.00000	5.88710	9.00000
$P_{D,18}$ (MW)	3.20000	3.20000	3.19213	3.20000	$P_{D,18}$ (MW)	3.20000	3.20000	3.19193	3.20000

Table 3.4 Comparing the best results in different optimisation algorithms of DSA scheme (Continued)

Double-Side Auction Scheme									
Variable	*Case 3.2a*				*Variable*	*Case 3.2b*			
	PSO	*BWO*	*GWO*	*WOA*		*PSO*	*BWO*	*GWO*	*WOA*
$P_{D,19}$ (MW)	9.50000	9.50000	9.46147	9.50000	$P_{D,19}$ (MW)	9.50000	9.50000	9.48952	9.50000
$P_{D,20}$ (MW)	2.20000	2.20000	2.19730	2.20000	$P_{D,20}$ (MW)	2.20000	2.20000	1.79252	2.20000
$P_{D,21}$ (MW)	17.50000	17.50000	17.16364	17.50000	$P_{D,21}$ (MW)	17.50000	17.50000	17.49509	17.50000
$P_{D,23}$ (MW)	3.20000	3.19998	3.17082	3.20000	$P_{D,23}$ (MW)	3.20000	3.20000	3.19496	3.20000
$P_{D,24}$ (MW)	8.70000	8.70000	8.70000	8.70000	$P_{D,24}$ (MW)	8.70000	8.70000	8.66107	8.70000
$P_{D,26}$ (MW)	0.00000	3.50000	0.13525	3.50000	$P_{D,26}$ (MW)	0.00000	3.50000	0.00221	0.34170
$P_{D,29}$ (MW)	2.40000	2.40000	2.38302	2.40000	$P_{D,29}$ (MW)	2.40000	2.40000	2.12447	2.40000
$P_{D,30}$ (MW)	10.60000	10.59999	3.05175	10.60000	$P_{D,30}$ (MW)	10.60000	0.07398	0.00000	10.60000
$f_{3.2a}$	**612.25805**	605.03273	605.73541	607.94252	$F_{3.2b}$	**602.36894**	593.78702	591.58698	597.80657
SW	**596.48420**	595.45684	596.37060	596.20107	***SW***	**602.36894**	593.78702	591.58698	597.80657
CE (t/h)	0.32233	0.31859	0.31263	0.32687	*CE (t/h)*	0.31577	0.31573	0.30763	0.29888
CCE ($/h)	9.99208	9.87640	9.69167	10.13300	*CCE ($/h)*	9.78887	9.78772	9.53667	9.26518
TCC ($/h)	**1,087.7486**	1,077.7954	1,101.4281	1,122.1867	***TCC ($/h)***	**1,083.0282**	1,058.8616	1,038.3661	1,138.7365

Table 3.5 Statistical comparison of case studies in different optimisation algorithms

Single-Side Auction Scheme								
Function	***Case 3.1a***				***Case 3.1b***			
Algorithm	*PSO*	*BWO*	*GWO*	*WOA*	*PSO*	*BWO*	*GWO*	*WOA*
Best	799.31549	800.19211	799.37519	799.55243	809.40759	810.11192	809.43595	809.68000
Worst	799.31552	803.75838	799.75972	800.53869	809.40763	819.88613	809.83685	810.78174
Average	799.31550	801.81634	799.52234	799.92350	809.40760	811.92861	809.63245	810.15134
Median	799.31550	801.84923	799.50325	799.90403	809.40760	811.47729	809.60973	810.10677
S.D.	0.00001	0.84418	0.11379	0.24268	0.00001	1.85885	0.10460	0.28039
Double-Side Auction Scheme								
Function	***Case 3.2a***				***Case 3.2b***			
Algorithm	*PSO*	*BWO*	*GWO*	*WOA*	*PSO*	*BWO*	*GWO*	*WOA*
Best	612.25805	605.03273	605.73541	607.94252	602.36894	593.78702	591.58698	597.80657
Worst	612.25775	437.43270	546.01117	576.92913	602.36832	431.38744	556.79640	558.24406
Average	612.25792	562.46385	583.00927	602.10967	602.36880	549.25934	576.03255	592.12092
Median	612.25792	576.79175	585.90390	603.55496	602.36885	560.70859	575.56178	594.60615
S.D.	0.00071	44.17016	14.18606	6.00640	0.00014	40.92580	9.99768	7.81242

3.6 Conclusion

This chapter introduces an enhanced optimal power dispatch and spot pricing framework that explicitly incorporates short-run carbon emission costs into the electricity market structure. The proposed model was rigorously tested on the IEEE 30-bus system using stochastic optimisation algorithms, namely PSO, BWO, GWO, and WOA. The findings reveal that embedding carbon emission costs directly into electricity spot pricing (Cases 3.1b and 3.2b) leads to a substantial reduction in carbon emissions compared to conventional pricing approaches (Cases 3.1a and 3.2a). In particular, the carbon-accounted scenarios resulted in lower carbon emissions and total consumer costs compared to the traditional cases, thereby validating the economic and environmental effectiveness of the proposed framework. Furthermore, the integration of the DSA scheme enhanced social welfare outcomes, highlighting the benefits of incorporating demand-side participation within carbon-aware market mechanisms. Among the optimisation techniques evaluated, PSO consistently exhibited superior performance, yielding lower objective function values, faster convergence, and greater computational efficiency compared to BWO, GWO, and WOA. These results underscore the robustness and applicability of PSO for real-time carbon-conscious electricity market dispatch.